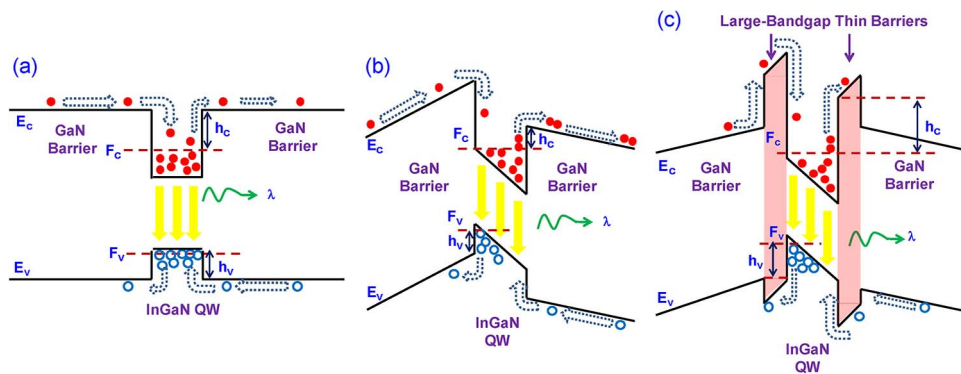


# Efficiency-Droop Suppression by Using Large-Bandgap AlGaN Thin Barrier Layers in InGaN Quantum-Well Light-Emitting Diodes

Volume 5, Number 2, April 2013

Guangyu Liu  
Jing Zhang  
Chee-Keong Tan  
Nelson Tansu



DOI: 10.1109/JPHOT.2013.2255028  
1943-0655/\$31.00 ©2013 IEEE

# Efficiency-Droop Suppression by Using Large-Bandgap AlGaInN Thin Barrier Layers in InGaN Quantum-Well Light-Emitting Diodes

Guangyu Liu, Jing Zhang, Chee-Keong Tan, and Nelson Tansu

Center for Photonics and Nanoelectronics, Department of Electrical and Computer Engineering, Lehigh University, Bethlehem, PA 18015 USA

DOI: 10.1109/JPHOT.2013.2255028  
1943-0655/\$31.00 ©2013 IEEE

Manuscript received February 15, 2013; revised March 12, 2013; accepted March 19, 2013. Date of publication March 27, 2013; date of current version April 8, 2013. This work was supported in part by the U.S. National Science Foundation under Grants ECCS 0701421, DMR 0907260, and ECCS 1028490, and in part by the Class of 1961 Professorship Fund. Corresponding authors: G. Liu and N. Tansu (e-mail: Gul308@Lehigh.Edu; Tansu@Lehigh.Edu).

**Abstract:** The electrical and optical characteristics of InGaN quantum-well light-emitting diodes with large-bandgap AlGaInN thin barriers were analyzed with the consideration of carrier transport effect for efficiency droop suppression. The lattice-matched AlGaInN quaternary alloys with different compositions, thicknesses, and positions were employed as thin barrier layers (1–2 nm) surrounding the InGaN QW in LED structures. The increased effective barrier heights of AlGaInN thin barrier led to suppression of carrier leakage as compared to conventional InGaN QW LEDs with GaN barrier only. The current work provides a comprehensive simulation taking into consideration the carrier transport in self-consistent manner, and the finding indicated the use of thin layers of AlGaInN or AlInN barriers as sufficient for suppressing the droop in InGaN-based QW LEDs. The efficiency of InGaN QW LED with the insertion of lattice-matched  $\text{Al}_{0.82}\text{In}_{0.18}\text{N}$  thin barrier layers showed the least droop phenomenon at high current density among the investigated LEDs. The thickness study indicated that a thin layer ( $< 2$  nm) of large-bandgap material in the barrier region was sufficient for efficiency droop suppression.

**Index Terms:** Efficiency droop, light-emitting diodes (LEDs), internal quantum efficiency (IQE), III-nitride, InGaN quantum wells (QWs), thin barrier design.

## 1. Introduction

III-Nitride semiconductors have been widely employed for energy-efficiency technologies, including light-emitting diodes (LEDs) for solid-state lighting [1]–[7], photovoltaics [8], and thermoelectric applications [9], [10]. Despite the tremendous progress achieved, several main challenges including “green gap” [2]–[4], [11] and “efficiency-droop” [2], [3], [5] in LEDs still hinder the further development of high brightness LEDs for general illumination. The efficiency of InGaN quantum well (QW) LEDs reduces significantly at high current density ( $J > 10\text{--}70$  A/cm<sup>2</sup>), which is referred as “efficiency-droop” phenomenon [2], [3], [5]. The efficiency-droop issue in InGaN QW LEDs becomes more severe, as the emission wavelength is pushed to longer spectral regime. The general illumination requires LEDs to be operated at  $J > 200$  A/cm<sup>2</sup>, which indicates the importance of addressing the efficiency droop issue.

Various mechanisms have been investigated to account for the efficiency droop phenomenon in nitride LEDs including: 1) carrier leakage [12]–[18], 2) Auger recombination process [19]–[22], 3) carrier loss via indirect absorption [23], 4) hole transport impediment [24]–[26], 5) junction heating effects [27]–[29], 6) large dislocation density [30], 7) decreased carrier localization at In-rich regions [31], and 8) current crowding effect [32]–[34]. Though the origin of the efficiency-droop phenomenon in InGaN-based LEDs remains controversial and inconclusive up till now, the primary reasons accounting for this issue have been mainly focused on the carrier density related mechanisms including Auger recombination and carrier leakage in III-nitrides. The Auger recombination coefficient  $C$  has been theoretically calculated and experimentally estimated for InGaN bulk materials, as well as InGaN/GaN QW systems [21]–[24], [35], [36]. A huge discrepancy of reported  $C$  values ranging from  $10^{-34} \text{ cm}^6 \text{ s}^{-1}$  to  $10^{-30} \text{ cm}^6 \text{ s}^{-1}$  still exists. The carrier escape processes have been investigated for the current injection efficiency quenching at high carrier density [15]–[18], which strongly indicates the assumption of unity injection efficiency at all current densities as invalid.

Various device structures have been explored to enhance the injection efficiency in InGaN QW LEDs [12]–[17], [25], [26], [34]–[46]. The suppression of efficiency droop using different barrier designs, electron blocking layers, and QW regions were performed by engineering the polarization field [12]–[14], [36]–[39], achieving uniform injection distribution across the active region [34], [40], [41], improving hole injection [42]–[46], and suppressing carrier leakage [15], [16]. Specifically, the large-bandgap materials were used as thick ( $\sim 12$  nm or thicker) barrier surrounding the QW [12], [13], [37], [40], [42] or thick electron blocking layers ( $\sim 20$  nm) [38], [39], [43], [44]. However, the use of thick layers of AlGaN or AlGaInN leads to challenging industrial implementation with possible contamination concern during the epitaxy of the active regions.

Recently, our works on the analytical study of current injection efficiency of InGaN QWs LEDs suggested that the use of thin ( $\sim 1$ – $2$  nm) large-bandgap barrier layers sandwiching the InGaN QWs have the potential to suppress the efficiency droop in the LEDs up to high current density [15], [16]. The driving force behind the carrier leakage process is related to the increase in thermionic carrier escape rate at high carrier/current injection level in polar InGaN-based QWs LEDs/lasers. The theoretical formulation and experimental works on the thermionic carrier escape rate, and its role in current injection quenching at high current density in QW lasers had been clarified [47]–[49]. Thus, the increased effective barrier height from the insertion of thin lattice-matched AlGaInN barriers surrounding InGaN QW was shown to significantly suppress the thermionic carrier escape process in the active region. In addition, the polarization-matched AlGaInN materials were used for efficiency-droop reduction previously [12], [13]. However, the use of thin layer of large-bandgap barrier for the carrier leakage suppression has not been extensively studied and optimized yet for enhancing the internal quantum efficiency (IQE) in nitride LEDs. Our analytical work [15], [16], [49] has also pointed out the advantage from the use of thin large-bandgap barriers, and this analytical method [15], [16] provides physically intuitive descriptions of the current injection efficiency quenching suppression in InGaN QWs with thin AlInN barriers.

In this paper, the characteristics of InGaN QW LEDs using large-bandgap AlGaInN thin ( $\sim 1$ – $2$  nm) barrier layers are analyzed with APSYS by taking into consideration the carrier transport effect. The modified drift-diffusion theory is used to account for the carrier transport effect, and the solutions are self-consistently coupled with the  $\mathbf{k} \cdot \mathbf{p}$  quantum mechanical solver for the calculation of band structures and radiative recombination rates [50]. The APSYS had been used in predicting the characteristics of III-Nitride-based LEDs [5], [26], [40]–[45]. The thin barrier layers are chosen as lattice-matched AlGaInN alloys with various compositions for practical experimental realization. The effects of the barrier height, thin barrier thickness, and barrier position on the performance of InGaN QW LEDs are analyzed. Single QW is used in our study instead of multiple QWs due to the nonuniformity issues in carrier distribution, as most of the carriers populate in the last QW near p-type side under electrical pumping [51].

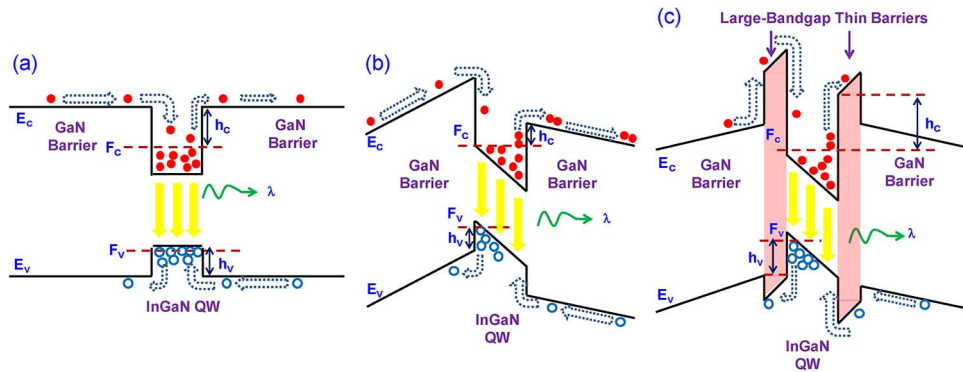


Fig. 1. Illustration of band structures and current/carrier flow in (a) nonpolar InGaN/GaN QW, (b) polar InGaN/GaN QW and (c) polar InGaN/GaN QW with large-bandgap thin barrier insertion.



Fig. 2. Schematics of InGaN QW LEDs consisting of 3 nm  $\text{In}_{0.28}\text{Ga}_{0.72}\text{N}$  QW with conventional 9 nm GaN barriers [LED (A)] and novel barrier design of 1 nm thin large-bandgap AlGaInN barrier together with 8 nm GaN thick barrier. The inserted table summarizes the material compositions and bandgaps of the thin lattice-matched AlGaInN barriers used in the study.

## 2. Concept of Novel Barrier Design in InGaN QW LED

III-nitride materials have large spontaneous and piezoelectric polarization fields, which result in severe band bending in the conventional InGaN/GaN QWs grown on c-plane substrates. Fig. 1 illustrates the schematics of band structures and current/carrier flow of (a) nonpolar InGaN/GaN QW, (b) polar c-plane InGaN/GaN QW, and (c) c-plane InGaN/GaN QW with large-bandgap thin barriers. The effective barrier heights for both electrons in conduction bands ( $h_c$ ) and holes in valence bands ( $h_v$ ) are reduced attributed to the polarization fields [see Fig. 1(a) and (b)]. Thus, the thermionic carrier escape rate from the QW to the barrier layers increases, especially at higher carrier/current injection. The insertion of large-bandgap thin barriers surrounding the InGaN QW [see Fig. 1(c)] results in increased effective barrier heights, which leads to thermionic carrier leakage suppression. The IQE of InGaN QW LEDs is the product of the injection efficiency and radiative efficiency, where the injection efficiency is defined as the ratio of the current that recombines in the active region over the total injected current. Thus, the use of large-bandgap thin barrier has the potential for suppressing the efficiency droop issue by maintaining high injection efficiency up to high current density.

Fig. 2 shows the schematics of LED structures used in the simulation with the corresponding thin large-bandgap lattice-matched barrier materials. The devices were designed to have rectangular geometry of  $400 \mu\text{m} \times 500 \mu\text{m}$  with a vertical injection configuration. The  $1\text{-}\mu\text{m}$ -thick n-GaN with  $n = 5 \times 10^{18} \text{ cm}^{-3}$  was used as the template of the devices. The active region consisted of a 3-nm-thick  $\text{In}_{0.28}\text{Ga}_{0.72}\text{N}$  QW ( $\lambda \sim 480\text{--}490 \text{ nm}$ ) sandwiched by AlGaInN thin barrier layers ( $\sim 1 \text{ nm}$ ) and GaN barriers ( $\sim 8 \text{ nm}$ ) for LED (B), (C), (D), and (E). The InGaN QW with GaN barrier ( $\sim 9 \text{ nm}$ ) only [LED (A)] was used as a reference. The background doping for GaN barriers, AlGaInN thin barriers, and InGaN QW layers was assumed as  $n = 5 \times 10^{16} \text{ cm}^{-3}$ . The 50-nm  $\text{Al}_{0.1}\text{Ga}_{0.9}\text{N}$  electron

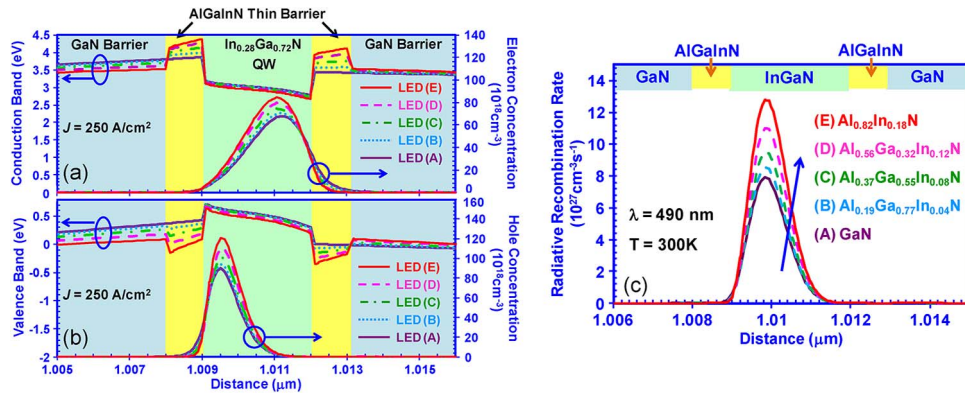


Fig. 3. (a) Conduction band structures and electron concentrations, (b) valence band structures and hole concentrations and (c) radiative recombination rates of 3 nm  $\text{In}_{0.28}\text{Ga}_{0.72}\text{N}$  QW LEDs with five different barrier designs at  $J = 250 \text{ A/cm}^2$ .

blocking layer (EBL) with p-type doping of  $3 \times 10^{17} \text{ cm}^{-3}$  was used, which is followed by 200-nm p-type GaN ( $p = 1.2 \times 10^{18} \text{ cm}^{-3}$ ). The p- and n-contacts were deposited on top and bottom of the p-GaN and n-GaN layers, respectively. The lattice constants of GaN, AlN, and InN are 3.189 Å, 3.112 Å, and 3.545 Å, respectively. The bandgap bowing parameters of InGaN/AlGaInN ternaries of 1.4 eV/0.8 eV/4.1 eV were used [15], and the corresponding bandgaps of AlGaInN thin barriers were calculated as 3.661 eV, 3.922 eV, 4.205 eV, and 4.464 eV at  $T = 300 \text{ K}$  for LEDs (B), (C), (D), and (E), respectively. The lattice-matched  $\text{Al}_{0.82}\text{In}_{0.18}\text{N}$  owns the great potential as the thin barrier material in LED (E) due to the largest bandgap available among the lattice-matched AlGaInN alloys and its relatively similar growth condition to the InGaInN alloy used in active region [52]. The material and band parameters used here were obtained from references [53], [54].

### 3. InGaN QW LEDs With Various AlGaInN Thin Barriers

#### 3.1. Characteristics of InGaN/AlGaInN QW LEDs at High Current Density

The characteristics of the four InGaN QW LEDs at high current density ( $J$ ) of  $250 \text{ A/cm}^2$  were compared. The screening caused by the defects was taken into account, and the surface charge density was assumed to be 50% of the calculated values. The band offset ratio ( $\Delta E_c : \Delta E_v$ ) was set as 70%:30% for all layers. Fig. 3 plots the band structures, carrier distributions, and radiative recombination rates in the layers of 3-nm  $\text{In}_{0.28}\text{Ga}_{0.72}\text{N}$  QW, 1-nm AlGaInN [or GaN for LED (A)] thin barriers, and 8-nm GaN thick barriers at  $J = 250 \text{ A/cm}^2$ . Fig. 3(a) focuses on the conduction bands and electron concentrations, and Fig. 3(b) focuses on the valence bands and hole concentrations. The insertions of large-bandgap thin barriers lead to the increases of effective barrier heights of electrons ( $h_c$ ) from 164 meV in LED (A) to 698 meV in LED (E) and effective barrier heights of holes ( $h_v$ ) from 171 meV in LED (A) to 410 meV in LED (E), respectively. Thus, the carrier leakage would potentially be suppressed. By using large-bandgap thin barriers from LEDs (A) to (E), the peak electron concentrations were increased from  $6.8 \times 10^{19} \text{ cm}^{-3}$  to  $8.4 \times 10^{19} \text{ cm}^{-3}$ , and the peak hole concentrations were increased from  $9 \times 10^{19} \text{ cm}^{-3}$  to  $12.1 \times 10^{19} \text{ cm}^{-3}$ , respectively. In addition, the carrier distributions were observed to align to the center of the QW resulting in stronger quantum confinement from the use of large-bandgap barrier, which, in turn, leads to the increase in radiative recombination rate. The radiative recombination rates of the four investigated LED structures across the active regions are presented in Fig. 3(c). Due to different carrier concentrations across the QW region, the radiative recombination rate as a function of the vertical position will provide the insights on the direct impact of increased carrier

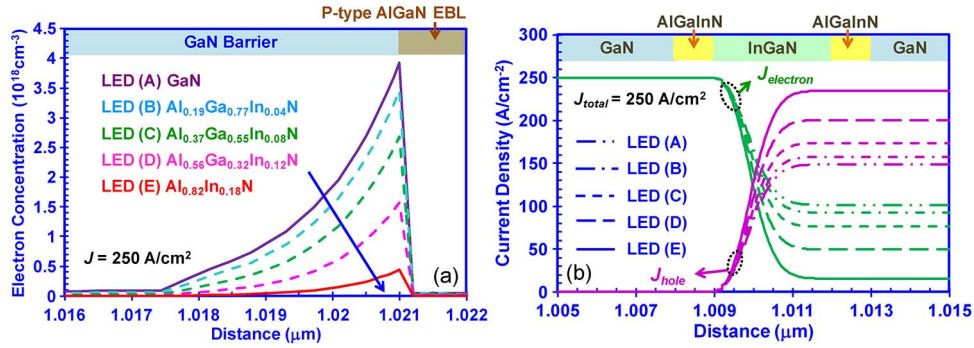


Fig. 4. (a) Electron concentrations in last GaN barriers and (b) the electron current densities ( $J_{\text{electron}}$ ) and hole current densities ( $J_{\text{hole}}$ ) across the active region of LED (A), (B), (C), (D) and (E) at  $J = 250 \text{ A/cm}^2$ .

concentrations and enhanced overlap in the active region. As the adjacent thin barrier changes from GaN in LED (A) to  $\text{Al}_{0.82}\text{In}_{0.18}\text{N}$  in LED (E), the peak radiative recombination rates inside the InGaIn QW were enhanced from  $7.9 \times 10^{27} \text{ cm}^{-3}\text{s}^{-1}$  to  $12.8 \times 10^{27} \text{ cm}^{-3}\text{s}^{-1}$ . The total radiative recombination rates were calculated as  $9.2 \times 10^{23} \text{ cm}^{-2}\text{s}^{-1}$  for LED (A) with GaN barrier only and  $14.6 \times 10^{23} \text{ cm}^{-2}\text{s}^{-1}$  for LED (E) with  $\text{Al}_{0.82}\text{In}_{0.18}\text{N}$  thin barrier. Thus, the light output power of LED with  $\text{Al}_{0.82}\text{In}_{0.18}\text{N}$  thin barrier is expected to be enhanced proportional to the increase in the integrated radiative recombination rate.

Due to the lower effective mass of electrons as compared with those of the holes, the carrier leakages were mainly attributed to the electron leakage in nitride-based QWs. To examine the current leakage, Fig. 4 shows the comparison of (a) the electron concentration in the last GaN barriers and (b) electron and hole current densities of the LEDs at  $J = 250 \text{ A/cm}^2$ . The peak electron concentrations were  $3.9 \times 10^{18} \text{ cm}^{-3}$ ,  $3.4 \times 10^{18} \text{ cm}^{-3}$ ,  $2.4 \times 10^{18} \text{ cm}^{-3}$ ,  $1.3 \times 10^{18} \text{ cm}^{-3}$ , and  $0.4 \times 10^{18} \text{ cm}^{-3}$  for LED (A), (B), (C), (D), and (E), respectively. The electron escape from the QW was suppressed from the increased barrier heights of AlGaInN thin barriers, leading to significantly reduced electron concentration in the last GaN barrier and AlGaIn EBL. To illustrate the current leakage suppression from the use of the thin AlGaInN barriers, the electron ( $J_{\text{electron}}$ ) and hole current densities ( $J_{\text{hole}}$ ) across the active region at  $J = 250 \text{ A/cm}^2$  were plotted in Fig. 4(b). Note that the n-contacts were placed at the bottom of the devices [see left side in Fig. 4(b)], and the p-contacts were placed on the top of the devices [see right side in Fig. 4(b)]. The hole currents were almost depleted after being transported through the active region, while the electron currents exhibited large leakage currents after the InGaIn QW layer. The electron leakage current densities were  $101 \text{ A/cm}^2$  for LED (A) with GaN barrier and  $16 \text{ A/cm}^2$  for LED (E) with  $\text{Al}_{0.82}\text{In}_{0.18}\text{N}$  thin barriers. The use of AlInN thin barriers results in 84.2% reduction of  $J_{\text{electron}}$  in the GaN barrier regions at  $J = 250 \text{ A/cm}^2$ .

### 3.2. Light Output Power and Electrical Characteristics of InGaIn/AlGaInN QW LEDs

The light output-power-current-voltage ( $L-I-V$ ) and IQE characteristics of the investigated LEDs [LEDs (A), (B), (C), (D), and (E)] as a function of current density were plotted in [see Fig. 5(a) and (b)], respectively. The extraction efficiency, monomolecular coefficient A, and Auger coefficient C were assumed as 70%,  $10^6 \text{ s}^{-1}$ , and  $10^{-34} \text{ cm}^6\text{s}^{-1}$ , respectively. The output power was observed as higher for InGaIn QW LEDs with AlGaInN thin barrier layers, as compared with that of LED (A), for all current densities. The output power was increased from 428 mW (A) to 687 mW (E) at  $J = 250 \text{ A/cm}^2$ . The  $I-V$  characteristics show a decreased turn-on voltage and a slight increased differential series resistance with increasing barrier height. The modification of the  $I-V$  for LED with AlGaInN thin barriers can be attributed to the change in the built-in potential in the barriers at high current density. The use of large-bandgap AlGaInN thin barrier layers considerably improves the IQE of LEDs at all current densities [see Fig. 5(b)].

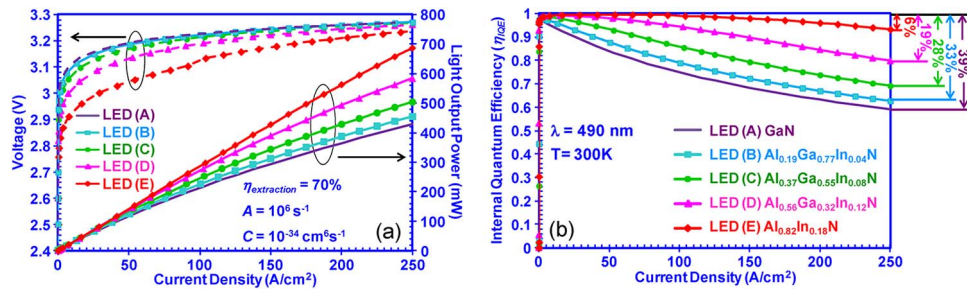


Fig. 5. (a) Light output powers and  $I$ - $V$  characteristics, (b) IQE ( $\eta_{\text{IQE}}$ ) for 3 nm In<sub>0.28</sub>Ga<sub>0.72</sub>N QW LEDs with five barrier designs of (A) GaN barriers, (B) Al<sub>0.19</sub>Ga<sub>0.77</sub>In<sub>0.04</sub>N thin barriers, (C) Al<sub>0.37</sub>Ga<sub>0.55</sub>In<sub>0.08</sub>N thin barriers, (D) Al<sub>0.56</sub>Ga<sub>0.32</sub>In<sub>0.12</sub>N thin barriers and (E) Al<sub>0.82</sub>In<sub>0.18</sub>N thin barrier as a function of current density.

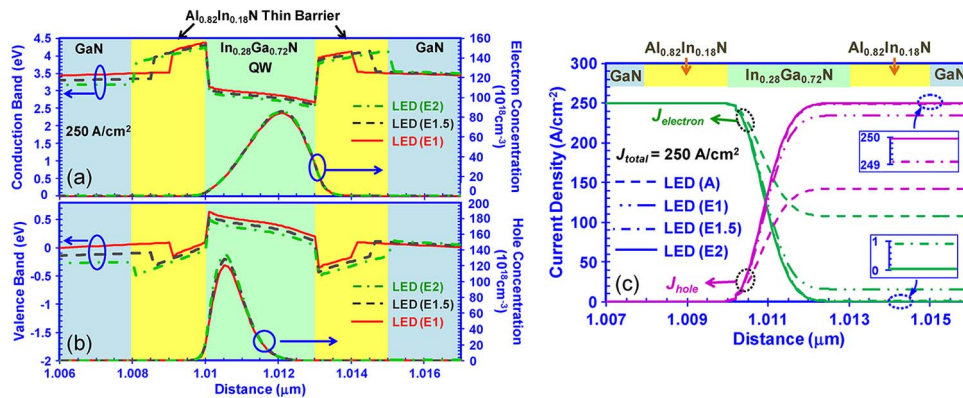


Fig. 6. (a) Conduction band structures and electron concentrations, (b) valence band structures and hole concentrations and (c) electron current densities and hole current densities across the QW active regions of 3 nm In<sub>0.28</sub>Ga<sub>0.72</sub>N QW LEDs with 1 nm (E1), 1.5 nm (E1.5) and 2 nm (E2) Al<sub>0.82</sub>In<sub>0.18</sub>N thin barriers at  $J = 250 \text{ A/cm}^2$ .

The efficiency-droop phenomenon was observed for all the five InGaN QW LEDs; however, the efficiency of LED (A) with GaN barrier started to reduce at lower current density as compared with the other four LEDs with AlGaInN thin barriers. The IQE of LED (A), (B), (C), (D), and (E) showed efficiency reduction of 39%, 33%, 26%, 16%, and 6% at  $J = 250 \text{ A/cm}^2$ , respectively, which confirms the suitability of this approach in suppressing efficiency droop in nitride LEDs. These four different AlGaInN compositions were chosen for providing guidance for experimentalists in implementing the thin barrier designs in device structures. Only recently, the growths of AlInN (with Al-content  $\sim 82\%$ ) with compatible active region growth temperature had been reported [52], and the use of AlGaInN thin barrier layers may also be beneficial in device implementation due to the more mature epitaxy of this alloy [26], [40].

#### 4. Characteristics of InGaN/AlInN QW LEDs With Different AlInN Thickness

To analyze the effect of the barrier thickness on the efficiency droop, we investigated the LED (E) with lattice-matched Al<sub>0.82</sub>In<sub>0.18</sub>N thin barrier of 1 nm [LED (E1)], 1.5 nm [LED (E1.5)], and 2 nm [LED (E2)] sandwiched by 8-nm GaN thick barriers. Fig. 6 plots the band structures, carrier concentrations, and current densities of the three LEDs at  $J = 250 \text{ A/cm}^2$ . Fig. 6(a) shows the conduction band and electron concentration profiles, while Fig. 6(b) shows the corresponding plots for valence band and hole concentration profiles. At  $J = 250 \text{ A/cm}^2$ , the electron concentrations in the InGaN QW layer show minimal improvement with increasing Al<sub>0.82</sub>In<sub>0.18</sub>N barrier thicknesses.

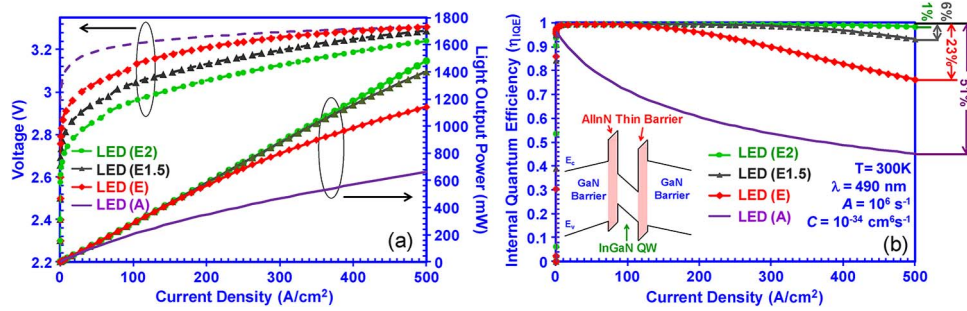


Fig. 7. (a) Light output powers and  $I$ - $V$  characteristics, and (b) IQE ( $\eta_{IQE}$ ) for 3 nm  $\text{In}_{0.28}\text{Ga}_{0.72}\text{N}$  QW LEDs with GaN barrier (A), 1 nm (E1), 1.5 nm (E1.5) and 2 nm (E2)  $\text{Al}_{0.82}\text{In}_{0.18}\text{N}$  thin barriers as a function of current density. The insertions show the schematic of InGaN QW LED with  $\text{Al}_{0.82}\text{In}_{0.18}\text{N}$  thin barriers. The maximum current density is extended to 500  $\text{A}/\text{cm}^2$ .

On the other hand, the peak hole concentration increases from  $1.21 \times 10^{20} \text{ cm}^{-3}$  to  $1.29 \times 10^{20} \text{ cm}^{-3}$  (and  $1.35 \times 10^{20} \text{ cm}^{-3}$ ), as the  $\text{Al}_{0.82}\text{In}_{0.18}\text{N}$  barrier thickness increases from 1 nm to 1.5 nm (and 2 nm), respectively. This finding indicates the further suppression of hole leakages in InGaN QW LEDs can be achieved by slight increase in the thin barrier thickness. Fig. 6(c) shows the electron current densities ( $J_{electron}$ ) and hole current densities ( $J_{hole}$ ) across the active region of the three InGaN QW LEDs with 1-nm, 1.5-nm, and 2-nm AlInN thin barriers at  $J = 250 \text{ A}/\text{cm}^2$ . The reference LED (A) with 10-nm GaN barrier was included for comparison purpose. The electron current densities after the active region were about 15.6  $\text{A}/\text{cm}^2$ , 0.9  $\text{A}/\text{cm}^2$ , 0.05  $\text{A}/\text{cm}^2$  for LED (E1), (E1.5), and (E2), respectively, while that of LED (A) was as high as 107.6  $\text{A}/\text{cm}^2$ . The results show that the electron leakage current has been substantially suppressed when  $d_{\text{AlInN}} \sim 1.5 \text{ nm}$ , and thick layer of large-bandgap barrier is not a necessity for leakage current suppression.

The  $L$ - $I$ - $V$  and IQE characteristics of LED (A), (E1), (E1.5), and (E2) were plotted as a function of current density (up to  $J = 500 \text{ A}/\text{cm}^2$ ) in Fig. 7(a) and (b), respectively. As shown in Fig. 7(a), the use of  $\text{Al}_{0.82}\text{In}_{0.18}\text{N}$  thin barrier with larger thickness leads to decreased forward voltage due to slight reduced polarization fields. The series resistances are comparable among the three LEDs with  $\text{Al}_{0.82}\text{In}_{0.18}\text{N}$  thin barrier. In addition, the light output power was significantly enhanced with the insertion of  $\text{Al}_{0.82}\text{In}_{0.18}\text{N}$  thin barrier with various thicknesses. The LED (E2) with 2-nm  $\text{Al}_{0.82}\text{In}_{0.18}\text{N}$  thin barrier exhibited the highest output power among these four LEDs at all current density. Specifically, at  $J = 500 \text{ A}/\text{cm}^2$ , the light output powers of LED (E1), (E1.5), and (E2) were 1140 mW, 1400 mW, and 1481 mW, which are significantly higher than that of LED (A) [661 mW]. Note that the difference between LED (E1.5) with 1.5-nm  $\text{Al}_{0.82}\text{In}_{0.18}\text{N}$  thin barrier and LED (E2) with 2-nm  $\text{Al}_{0.82}\text{In}_{0.18}\text{N}$  thin barrier was minimal. The efficiency droop was significantly reduced by the insertion of lattice matched AlInN thin barriers surrounding the InGaN QW from the results of Fig. 7(b). The reduction of IQEs of LED (A), (E1), (E1.5), and (E2) were 51%, 23%, 6%, and 1% at  $J = 500 \text{ A}/\text{cm}^2$ , respectively. Both LED (E1.5) with 1.5-nm  $\text{Al}_{0.82}\text{In}_{0.18}\text{N}$  thin barrier and (E2) with 2-nm  $\text{Al}_{0.82}\text{In}_{0.18}\text{N}$  thin barrier maintained the high IQE level (IQE > 90%) till very high current density ( $J > 500 \text{ A}/\text{cm}^2$ ), while the conventional InGaN QW with GaN barrier (LED (A)) show droop phenomenon at very low current density ( $J > 10 \text{ A}/\text{cm}^2$ ). The finding confirmed that the use of a thin layer (< 2 nm) of large-bandgap barrier is sufficient in efficiency droop suppression.

## 5. InGaN/AlInN QW LEDs With Different Position of AlInN Thin Barriers

To study the effect of the thin barrier position, we compared the characteristics of three types of InGaN QW LEDs with 1-nm  $\text{Al}_{0.82}\text{In}_{0.18}\text{N}$  thin barrier at different positions. Fig. 8 shows the band structures and corresponding quasi-Fermi levels of LED (E), LED (ER), and LED (EL) at  $J = 250 \text{ A}/\text{cm}^2$ . The LED (E), as described in the earlier discussion and shown in Fig. 8(a), has lattice-matched  $\text{Al}_{0.82}\text{In}_{0.18}\text{N}$  thin barrier on both sides of InGaN QW layer. In addition, LED (ER) in

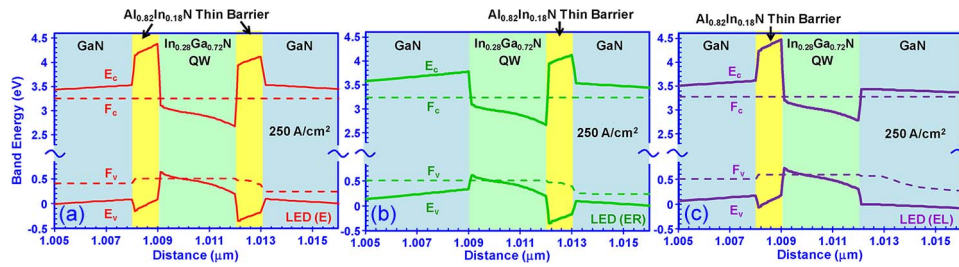


Fig. 8. Band structures and corresponding quasi Fermi levels of (a) LED (E) with 1 nm  $\text{Al}_{0.82}\text{In}_{0.18}\text{N}$  thin barriers on both sides of 3 nm  $\text{In}_{0.28}\text{Ga}_{0.72}\text{N}$  QW, (b) LED (ER) with 1 nm  $\text{Al}_{0.82}\text{In}_{0.18}\text{N}$  thin barriers on the right-hand side of 3 nm  $\text{In}_{0.28}\text{Ga}_{0.72}\text{N}$  QW and (c) LED (EL) with 1 nm  $\text{Al}_{0.82}\text{In}_{0.18}\text{N}$  thin barriers on the left-hand side of 3 nm  $\text{In}_{0.28}\text{Ga}_{0.72}\text{N}$  QW at  $J = 250 \text{ A/cm}^2$ .

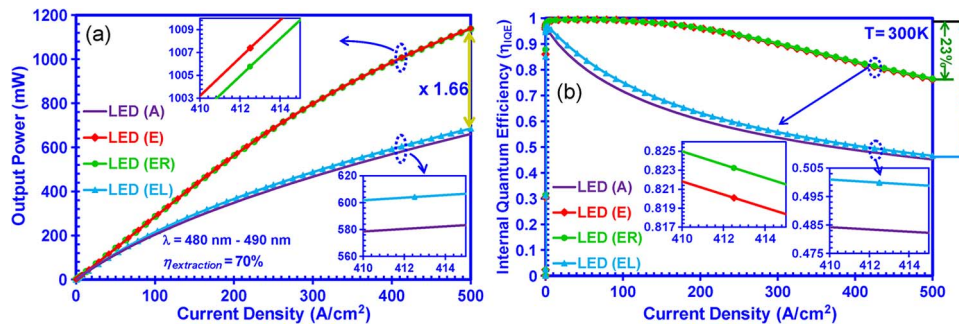


Fig. 9. (a) Light output power and (b) IQE ( $\eta_{\text{intQE}}$ ) of LED (A) with GaN barrier, LED (E) with  $\text{Al}_{0.82}\text{In}_{0.18}\text{N}$  thin barriers on both sides, LED (ER) with  $\text{Al}_{0.82}\text{In}_{0.18}\text{N}$  thin barriers on the right-hand side and LED (EL) with  $\text{Al}_{0.82}\text{In}_{0.18}\text{N}$  thin barriers on the left-hand side of 3 nm  $\text{In}_{0.28}\text{Ga}_{0.72}\text{N}$  QW, respectively.

Fig. 8(b) has only the  $\text{Al}_{0.82}\text{In}_{0.18}\text{N}$  thin barrier on the right-hand side of InGaN QW for electron leakage suppression, and LED (EL) in Fig. 8(c) has the  $\text{Al}_{0.82}\text{In}_{0.18}\text{N}$  thin barrier on the left-hand side of InGaN QW for hole leakage suppression. Note that the electrons were injected from the left-hand side near the n-type GaN and the holes were injected from the right-hand side near the p-type GaN. The quasi-Fermi levels for electrons in conduction bands ( $F_c$ ) remained relatively unchanged for the three LEDs, while the quasi-Fermi levels for holes in valence bands ( $F_v$ ) showed slight increase at the  $\text{Al}_{0.82}\text{In}_{0.18}\text{N}$  thin barrier layer.

Fig. 9(a) and (b) shows the light output powers and IQE of LEDs (E), (ER), (EL), and (A) up till  $J = 500 \text{ A/cm}^2$  ( $\lambda_{\text{peak}} \sim 480 - 490 \text{ nm}$ ) at  $T = 300 \text{ K}$ , respectively. The powers and IQE of LED (EL) were similar to these of LED (A), and LED (ER) showed similar performance with LED (E). The insets show the enlarged curves where the light output power of LED (ER) as slightly lower than that of LED (E) due to the hole leakages. Similarly, the light output power of LED (EL) is slightly higher than that of LED (A) due to the hole leakage suppression. The output power of LED (ER) was about 1.66 times higher than that of LED (EL) at  $J = 500 \text{ A/cm}^2$ , which is about 1.72 times higher than that of the reference LED (A), as shown in Fig. 9(a). In Fig. 9(b), the reductions of IQE at  $J = 500 \text{ A/cm}^2$  were 23.1%, 23.3%, 50.6%, and 53% for LED (E), LED (ER), LED (EL), and LED (A), respectively. These results are in good agreement with the finding that indicated the electron leakage as the dominant carrier loss process resulting to efficiency-droop phenomenon. In addition to surrounding both sides of the QW with thin large-bandgap barriers, the increase in injection efficiency and reduction of efficiency droop can also be realized by the insertion of a thin layer of large-bandgap barrier on the path of electron leakage near the p-GaN side. The finding indicates the importance of electron leakage suppression in enhancing the efficiency of InGaN QW LEDs at high current density, and it provides a more practical device structure for experiments.

## 6. Summary

In summary, we have analyzed InGaN QW LEDs with the insertion of a thin large-bandgap AlGaInN barrier layers for efficiency-droop suppression in nitride-based LEDs. The simulation has been carried out by taking into consideration the polarization field of III-nitrides, carrier screening, and carrier transport effect. The current numerical work provides a good agreement to the previous finding based on the more physically intuitive analytical model [15], [16]. In comparison with conventional InGaN QW LEDs with GaN barrier only, the InGaN QW LEDs with lattice-matched AlGaInN thin barriers exhibited improved carrier confinement and reduction in efficiency droop. The key factor leading to the droop suppression in our approach was attributed to the suppression of thermionic carrier escape process in the InGaN-based QWs by increasing the effective barrier heights via thin large-bandgap barrier designs. There exists a balance of the carrier capture and thermionic escape processes in the optimization of current injection efficiency in QW lasers / LEDs. The current injection efficiency in QW lasers/LEDs is inversely proportional to the ratio of carrier capture time and thermionic carrier escape time ( $\tau_{\text{cap}}/\tau_{\text{thermionic}}$ ) [49]. The introduction of the thin large-bandgap barrier layer will primarily affect the quantum mechanical capture process ( $\tau_{\text{cap\_QM}}$ ), which is expected to only result in relatively minor correction to the carrier capture lifetime [48], [57].

In this paper, the large-bandgap AlInN barrier layers have been designed with the goal of minimizing the layer thickness down to  $\sim 1\text{--}2$  nm, in order to ensure practical experimental implementation with minimal impact of the material quality. In addition, we have also found that the use of barrier to the right side of the QW (for blocking the electron escape process) played the most important role in maintaining high injection efficiency in the QW. Recent experimental works on InGaN QW LEDs with polarization-matched quaternary AlGaInN thick barriers ( $\sim 10\text{--}12$  nm) have been reported by using metalorganic chemical vapor deposition (MOCVD) [13], [40], [55], [56]. The results indicated that the incorporation of AlGaInN thick barrier layers could be realized without adversely impacting materials quality and optical properties of InGaN QW LEDs [13], [40], [55], [56]. In our concept, the use of much thinner ( $\sim 1\text{--}2$  nm) large-bandgap barriers of AlGaInN or AlInN resulted in suppression of efficiency-droop in nitride-based LEDs. Our recent finding also indicated that the growth condition for AlInN is compatible to that of InGaN active regions [52]. Thus, the incorporation of thin ( $\sim 1\text{--}2$  nm) ternary AlInN or quaternary AlGaInN barrier materials in InGaN-based QW active regions will be compatible with the LED MOCVD manufacturing process.

## Acknowledgment

The work was previously presented in IEEE Photonics Conference 2012 (Burlingame, CA, September 2012).

---

## References

- [1] S. Nakamura, M. Senoh, S. Nagahama, N. Iwasa, T. Yamada, T. Matsushita, H. Kiyoku, and Y. Sugimoto, "InGaN-based multi-quantum-well-structure laser diodes," *Jpn. J. Appl. Phys.*, vol. 35, no. 1B, pp. L74–L76, Jan. 15, 1996.
- [2] M. R. Krames, O. B. Shchekin, R. Mueller-Mach, G. O. Mueller, L. Zhou, G. Harbers, and M. G. Craford, "Status and future of high-power light-emitting diodes for solid-state lighting," *J. Display Technol.*, vol. 3, no. 2, pp. 160–175, Jun. 2007.
- [3] M. H. Crawford, "LEDs for solid-state lighting: Performance challenges and recent advances," *IEEE J. Sel. Topics Quantum Electron.*, vol. 15, no. 4, pp. 1028–1040, Jul./Aug. 2009.
- [4] H. P. Zhao, G. Y. Liu, J. Zhang, J. D. Poplawsky, V. Dierolf, and N. Tansu, "Approaches for high internal quantum efficiency green InGaN light-emitting diodes with large overlap quantum wells," *Opt. Exp.*, vol. 19, no. S4, pp. A991–A1007, Jul. 2011.
- [5] J. Piprek, "Efficiency droop in nitride-based light-emitting diodes," *Phys. Stat. Sol. A, Appl. Mater. Sci.*, vol. 207, no. 10, pp. 2217–2225, Oct. 2010.
- [6] X. Li, S. Kim, E. E. Reuter, S. G. Bishop, and J. J. Coleman, "The incorporation of arsenic in GaN by metalorganic chemical vapor deposition," *Appl. Phys. Lett.*, vol. 72, no. 16, pp. 1990–1992, Apr. 1998.
- [7] I. H. Brown, P. Blood, P. M. Smowton, J. D. Thomson, S. M. Olaizola, A. M. Fox, P. J. Parbrook, and W. W. Chow, "Time evolution of the screening of piezoelectric fields in InGaN quantum wells," *IEEE J. Quantum Electron.*, vol. 42, no. 12, pp. 1202–1208, Nov./Dec. 2006.
- [8] R. Dahal, B. Pantha, J. Li, J. Y. Lin, and H. X. Jiang, "InGaN/GaN multiple quantum well solar cells with long operating wavelengths," *Appl. Phys. Lett.*, vol. 94, no. 6, pp. 063505-1–063505-3, Feb. 2009.

- [9] B. N. Pantha, I. Feng, K. Aryal, J. Li, J. Y. Lin, and H. X. Jiang, "Erbium-doped allInGaN alloys as high-temperature thermoelectric materials," *Appl. Phys. Exp.*, vol. 4, no. 5, pp. 051001-1–051001-3, May 2011.
- [10] J. Zhang, S. Kutlu, G. Y. Liu, and N. Tansu, "High-temperature characteristics of seebeck coefficients for AllnN alloys grown by metalorganic vapor phase epitaxy," *J. Appl. Phys.*, vol. 110, no. 4, pp. 043710-1–043710-6, Aug. 2011.
- [11] R. M. Farrell, E. C. Young, F. Wu, S. P. DenBaars, and J. S. Speck, "Materials and growth issues for high-performance nonpolar and semipolar light-emitting devices," *Semicond. Sci. Technol.*, vol. 27, no. 2, p. 024001, Feb. 2012.
- [12] M. H. Kim, M. F. Schubert, Q. Dai, J. K. Kim, E. F. Schubert, J. Piprek, and Y. Park, "Origin of efficiency droop in GaN-based light-emitting diodes," *Appl. Phys. Lett.*, vol. 91, no. 18, pp. 183507-1–183507-3, Oct. 2007.
- [13] M. F. Schubert, J. Xu, J. K. Kim, E. F. Schubert, M. H. Kim, S. Yoon, S. M. Lee, C. S. Sone, T. Sakong, and Y.-J. J. Park, "Polarization-matched GaInN/AlGaInN multi-quantum-well light-emitting diodes with reduced efficiency droop," *Appl. Phys. Lett.*, vol. 93, no. 4, pp. 041102-1–041102-3, Jul. 2008.
- [14] J. R. Xu, M. F. Schubert, A. N. Noemaun, D. Zhu, J. K. Kim, E. F. Schubert, M.-H. H. Kim, H. J. Chung, S. Yoon, C. S. Sone, and Y.-J. J. Park, "Reduction in efficiency droop, forward voltage, ideality factor, and wavelength shift in polarization-matched GaInN/GaN multi-quantum-well light-emitting diodes," *Appl. Phys. Lett.*, vol. 94, no. 1, pp. 011113-1–011113-3, Jan. 2009.
- [15] H. P. Zhao, G. Y. Liu, R. A. Arif, and N. Tansu, "Current injection efficiency quenching leading to efficiency droop in InGaN quantum well light-emitting diodes," *Solid State Electron.*, vol. 54, no. 10, pp. 1119–1124, Oct. 2010.
- [16] H. P. Zhao, G. Y. Liu, J. Zhang, R. A. Arif, and N. Tansu, "Analysis of internal quantum efficiency and current injection efficiency in III-nitride light-emitting diodes," *J. Display Technol.*, vol. 9, no. 4, pp. 212–225, Apr. 2013.
- [17] G.-B. Lin, D. Meyaard, J. H. Cho, E. F. Schubert, H. W. Shim, and C. S. Sone, "Analytic model for the efficiency droop in semiconductors with asymmetric carrier-transport properties based on drift-induced reduction of injection efficiency," *Appl. Phys. Lett.*, vol. 100, no. 16, pp. 161106-1–161106-4, Apr. 2012.
- [18] J. Wang, L. Wang, L. Wang, Z. Hao, Y. Luo, A. Dempewolf, M. Müller, F. Bertram, and J. Christen, "An improved carrier rate model to evaluate internal quantum efficiency and analyze efficiency droop origin of InGaN based light-emitting diodes," *J. Appl. Phys.*, vol. 112, no. 2, pp. 023107-1–023107-6, Jul. 2012.
- [19] I. E. Titkov, D. A. Sannikov, Y.-M. Park, and J.-K. Son, "Blue light emitting diode internal and injection efficiency," *AIP Adv.*, vol. 2, no. 3, pp. 032117-1–032117-4, Sep. 2012.
- [20] Y. C. Shen, G. O. Mueller, S. Watanabe, N. F. Gardner, A. Munkholm, and M. R. Krames, "Auger recombination in InGaN measured by photoluminescence," *Appl. Phys. Lett.*, vol. 91, no. 14, pp. 141101-1–141101-3, Oct. 2007.
- [21] K. T. Delaney, P. Rinke, and C. G. Van de Walle, "Auger recombination rates in nitrides from first principles," *Appl. Phys. Lett.*, vol. 94, no. 19, pp. 191109-1–191109-3, May 2009.
- [22] E. Kioupakis, P. Rinke, K. T. Delaney, and C. G. Van de Walle, "Indirect auger recombination as a cause of efficiency droop in nitride light-emitting diodes," *Appl. Phys. Lett.*, vol. 98, no. 16, pp. 161107-1–161107-3, Apr. 2011.
- [23] E. Kioupakis, P. Rinke, A. Schleife, F. Bechstedt, and C. G. Van de Walle, "Free-carrier absorption in nitrides from first principles," *Phys. Rev. B, Condens. Matter*, vol. 81, no. 24, pp. 241201-1–241201-4, Jun. 2010.
- [24] J. Q. Xie, X. Ni, Q. Fan, R. Shimada, Ü. Özgür, and H. Morkoç, "On the efficiency droop in InGaN multiple quantum well blue light emitting diodes and its reduction with p-doped quantum well barriers," *Appl. Phys. Lett.*, vol. 93, no. 12, pp. 121107-1–121107-3, Sep. 2008.
- [25] X. Ni, Q. Fan, R. Shimada, Ü. Özgür, and H. Morkoç, "Reduction of efficiency droop in InGaN light emitting diodes by coupled quantum wells," *Appl. Phys. Lett.*, vol. 93, no. 17, pp. 171113-1–171113-3, Oct. 2008.
- [26] C. H. Wang, S. P. Chang, W. T. Chang, J. C. Li, Y. S. Lu, Z. Y. Li, H. C. Yang, H. C. Kuo, T. C. Lu, and S. C. Wang, "Efficiency droop alleviation in InGaN/GaN light-emitting diodes by graded-thickness multiple quantum wells," *Appl. Phys. Lett.*, vol. 97, no. 18, pp. 181101-1–181101-3, Nov. 2010.
- [27] A. A. Efremov, N. I. Bochkareva, R. I. Gorbunov, D. A. Lavrinovich, Y. T. Rebane, D. V. Tarkhin, and Y. G. Shreter, "Effect of the joule heating on the quantum efficiency and choice of thermal conditions for high-power blue InGaN/GaN LEDs," *Semiconductors*, vol. 40, no. 5, pp. 605–610, May 2006.
- [28] W. W. Chow, M. H. Crawford, J. Y. Tsao, and M. Kneissl, "Internal efficiency of InGaN light-emitting diodes: Beyond a quasiequilibrium model," *Appl. Phys. Lett.*, vol. 97, no. 12, pp. 121105-1–121105-3, Sep. 2010.
- [29] J. Hader, J. V. Moloney, and S. W. Koch, "Temperature-dependence of the internal efficiency droop in GaN-based diodes," *Appl. Phys. Lett.*, vol. 99, no. 18, pp. 181127-1–181127-3, Oct. 2011.
- [30] M. F. Schubert, S. Chhajed, J. K. Kim, E. Fred Schubert, D. D. Koleske, M. H. Crawford, S. R. Lee, A. J. Fischer, G. Thaler, and M. A. Banas, "Effect of dislocation density on efficiency droop in GaInN/GaN light-emitting diodes," *Appl. Phys. Lett.*, vol. 91, no. 23, pp. 231114-1–231114-3, Dec. 2007.
- [31] S. F. Chichibu, T. Azuhata, M. Sugiyama, T. Kitamura, Y. Ishida, H. H. Okumura, T. Nakanishi, T. Sota, and T. Mukai, "Optical and structural studies in InGaN quantum well structure laser diodes," *J. Vac. Sci. Technol. B*, vol. 19, no. 6, pp. 2177–2183, Nov. 2001.
- [32] X. Guo and E. F. Schubert, "Current crowding in GaN/InGaN light emitting diodes on insulating substrates," *J. Appl. Phys.*, vol. 90, no. 8, pp. 4191–4195, Oct. 2001.
- [33] V. K. Malyutenko, S. S. Bolgov, and A. D. Podoltsev, "Current crowding effect on the ideality factor and efficiency droop in blue lateral InGaN/GaN light emitting diodes," *Appl. Phys. Lett.*, vol. 97, no. 25, pp. 251110-1–251110-3, Dec. 2010.
- [34] Y. Y. Kudryk and A. V. Zinovchuk, "Efficiency droop in InGaN/GaN multiple quantum well light-emitting diodes with nonuniform current spreading," *Semicond. Sci. Technol.*, vol. 26, no. 9, pp. 095007-1–095007-5, Sep. 2011.
- [35] J. Hader, J. V. Moloney, B. Pasenow, S. W. Koch, M. Sabathil, N. Linder, and S. Lutgen, "On the importance of radiative and auger losses in GaN-based quantum wells," *Appl. Phys. Lett.*, vol. 92, no. 26, pp. 261103-1–261103-3, Jun. 2008.
- [36] H. J. Chung, R. J. Choi, M. H. Kim, J. W. Han, Y. M. Park, Y. S. Kim, H. S. Paek, C. S. Sone, Y. J. Park, J. K. Kim, and E. Fred Schubert, "Improved performance of GaN-based blue light emitting diodes with InGaN/GaN multilayer barriers," *Appl. Phys. Lett.*, vol. 95, no. 24, pp. 241109-1–241109-3, Dec. 2009.
- [37] J.-Y. Chang and Y.-K. Kuo, "Influence of polarization-matched AlGaInN barriers in blue InGaN light-emitting diodes," *Opt. Lett.*, vol. 37, no. 9, pp. 1574–1576, May 2012.

- [38] S. Choi, H. J. Kim, S.-S. Kim, J. Liu, J. Kim, J.-H. Ryou, R. D. Dupuis, A. M. Fischer, and F. A. Ponce, "Improvement of peak quantum efficiency and efficiency droop in III-nitride visible light-emitting diodes with an InAlN electron-blocking layer," *Appl. Phys. Lett.*, vol. 96, no. 22, pp. 221105-1–221105-3, May 2010.
- [39] H. J. Kim, S. Choi, S.-S. Kim, J.-H. Ryou, P. D. Yoder, R. D. Dupuis, A. M. Fischer, K. W. Sun, and F. A. Ponce, "Improvement of quantum efficiency by employing active-layer-friendly lattice-matched InAlN electron blocking layer in green light-emitting diodes," *Appl. Phys. Lett.*, vol. 96, no. 10, pp. 101102-1–101102-3, Mar. 2010.
- [40] P. M. Tu, C. Y. Chang, S. C. Huang, C. H. Chiu, J. R. Chang, W. T. Chang, D. S. Wu, H.-W. Zan, C.-C. Lin, H.-C. Kuo, and C.-P. Hsu, "Investigation of efficiency droop for InGaN-based UV light-emitting diodes with InAlGaN barrier," *Appl. Phys. Lett.*, vol. 98, no. 21, pp. 211107-1–211107-3, May 2011.
- [41] Y.-K. Kuo, T.-H. Wang, J.-Y. Chang, and M.-C. Tsai, "Advantages of InGaN light-emitting diodes with GaN-InGaN-GaN barriers," *Appl. Phys. Lett.*, vol. 99, no. 9, pp. 091107-1–091107-3, Aug. 2011.
- [42] J.-Y. Chang, M.-C. Tsai, and Y.-K. Kuo, "Advantages of blue InGaN light-emitting diodes with AlGaN barriers," *Opt. Lett.*, vol. 35, no. 9, pp. 1368–1370, May 2010.
- [43] Y. K. Kuo, J. Y. Chang, and M. C. Tsai, "Enhancement in hole-injection efficiency of blue InGaN light-emitting diodes from reduced polarization by some specific designs for the electron blocking layer," *Opt. Lett.*, vol. 35, no. 19, pp. 3285–3287, Oct. 2010.
- [44] C. H. Wang, C. C. Ke, C. Y. Lee, S. P. Chang, W. T. Chang, J. C. Li, Z. Y. Li, H. C. Yang, H. C. Kuo, T. C. Lu, and S. C. Wang, "Hole injection and efficiency droop improvement in InGaN/GaN light-emitting diodes by band-engineered electron blocking layer," *Appl. Phys. Lett.*, vol. 97, no. 26, pp. 261103-1–261103-3, Dec. 2010.
- [45] C. H. Wang, S. P. Chang, P. H. Ku, J. C. Li, Y. P. Lan, C. C. Lin, H. C. Yang, H. C. Kuo, T. C. Lu, S. C. Wang, and C. Y. Chang, "Hole transport improvement in InGaN/GaN light-emitting diodes by graded-composition multiple quantum barriers," *Appl. Phys. Lett.*, vol. 99, no. 17, pp. 171106-1–171106-3, Oct. 2011.
- [46] Y.-K. Kuo, T.-H. Wang, and J.-Y. Chang, "Blue InGaN light-emitting diodes with multiple GaN-InGaN barriers," *IEEE J. Quantum Electron.*, vol. 48, no. 7, pp. 946–951, Jul. 2012.
- [47] N. Tansu, J. Y. Yeh, and L. J. Mawst, "Experimental evidence of carrier leakage in InGaAsN quantum well lasers," *Appl. Phys. Lett.*, vol. 83, no. 11, pp. 2112–2114, Sept. 2003.
- [48] L. Xu, D. Patel, C. S. Menoni, J. Yeh, L. J. Mawst, and N. Tansu, "Experimental evidence of the impact of nitrogen on carrier capture and escape times in InGaAsN / GaAs single quantum well," *IEEE Photon. J.*, vol. 4, no. 6, pp. 2262–2271, Dec. 2012.
- [49] N. Tansu and L. J. Mawst, "Current injection efficiency of 1300-nm InGaAsN quantum-well lasers," *J. Appl. Phys.*, vol. 97, no. 5, pp. 054502-1–054502-18, Mar. 2005.
- [50] APSYS, Burnaby, BC, Canada. [Online]. Available: <http://www.crosslight.com>
- [51] A. David, M. J. Grundmann, J. F. Kaeding, N. F. Gardner, T. G. Mihopoulos, and M. R. Krames, "Carrier distribution in (0001) InGaN/GaN multiple quantum well light-emitting diodes," *Appl. Phys. Lett.*, vol. 92, no. 5, pp. 053502-1–053502-3, Feb. 2008.
- [52] G. Y. Liu, J. Zhang, X. H. Li, G. S. Huang, T. Paskova, K. R. Evans, H. P. Zhao, and N. Tansu, "Metalorganic vapor phase epitaxy and characterizations of nearly-lattice-matched AlInN alloys on GaN / sapphire templates and free-standing GaN substrates," *J. Cryst. Growth*, vol. 340, no. 1, pp. 66–73, Feb. 2012.
- [53] I. Vurgaftman and J. R. Meyer, "Band parameters for nitrogen-containing semiconductors," *J. Appl. Phys.*, vol. 94, no. 6, pp. 3675–3696, Sep. 2003.
- [54] I. Vurgaftman and J. R. Meyer, *Chapter 2 in nitride semiconductor devices*, J. Piprek, Ed. Hoboken, NJ, USA: Wiley, 2007.
- [55] A. Knauer, H. Wenzel, T. Kolbe, S. Einfeldt, M. Weyers, M. Kneissl, and G. Trankle, "Effect of the barrier composition on the polarization fields in near UV InGaN light emitting diodes," *Appl. Phys. Lett.*, vol. 92, no. 19, pp. 191912-1–191912-3, May 2008.
- [56] J. J. Wu, G. Y. Zhang, X. L. Liu, Q. S. Zhu, Z. Wang, Q. Jia, and L. Guo, "Effect of an indium-doped barrier on enhanced near-ultraviolet emission from InGaN/AlGaIn: In multiple quantum wells grown on Si(111)," *Nanotechnology*, vol. 18, no. 1, pp. 015402-1–015402-5, Jan. 2007.
- [57] Y. C. Lu, C. Y. Chen, H. C. Wang, C. C. Yang, and Y. C. Cheng, "Carrier trapping effects on photoluminescence decay time in InGaN/GaN quantum wells with nanocluster structures," *J. Appl. Phys.*, vol. 101, no. 6, pp. 063511-1–063511-7, Mar. 2007.